Structure and Stereodynamics of $Fe(CO)_4L$ Complexes (L = $P(o\text{-tolyl})_3$, $As(o\text{-tolyl})_3$, $P(o\text{-tolyl})_2CH_2Ph$, $(o\text{-tolyl})_2PP(o\text{-tolyl})_2$)

James A. S. Howell,*,† Michael G. Palin,† Patrick McArdle,‡ Desmond Cunningham,‡ Zeev Goldschmidt,§ Hugo E. Gottlieb,§ and Daphna Hezroni-Langerman§

Chemistry Departments, University College, Galway, Ireland, Keele University, Keele, Staffordshire ST5 5BG, U.K., and Bar Ilan University, Ramat Gan 52100, Israel

Received November 24, 1992

The crystal structures and variable-temperature NMR spectra of $(CO)_4FeP(o\text{-tolyl})_3$, $(CO)_4FeAs(o\text{-tolyl})_3$, $(CO)_4FeP(o\text{-tolyl})_2CH_2Ph$, and $(CO)_4Fe(o\text{-tolyl})_2PP(o\text{-tolyl})_2$ (**1a–d**) are reported. In the solid state, complexes **1a–c** contain the phosphine in an axial position of the trigonal bipyramid; complex **1d** is equatorially substituted in the solid state but exists as an axial/equatorial mixture in solution. All complexes exhibit P–C restricted rotation, which in the case of **1a** may be linked to axial/equatorial CO exchange. Crystallographic data: **1a**, $C_{25}H_{21}FeO_4P$, monoclinic, $P2_1/n$, a = 10.188(3) Å, b = 10.429(2) Å, c = 21.755(6) Å, β = 99.79(2)°, Z = 4; **1b**, $C_{25}H_{21}AsFeO_4$, monoclinic, $P2_1/n$, a = 10.265(2) Å, b = 10.517(1) Å, c = 21.679(3) Å, β = 99.16(2)°, Z = 4; **1c**, $C_{25}H_{21}FeO_4P$, triclinic, $P\bar{1}$, a = 9.618(3) Å, b = 15.282(3) Å, c = 17.130(5) Å, α = 66.92(2)°, β = 79.51(2)°, γ = 86.42(2)°, Z = 4; **1d**, $C_{32}H_{38}FeO_4P_2$, orthorhombic, $Pbca$, a = 15.947(6) Å, b = 20.009(3) Å, c = 15.470(4) Å, Z = 8.

Introduction

As ancillary ligands in transition metal complexes, phosphines provide great potential for control of structure and activity through variation of both steric and electronic properties. Of particular relevance to catalysis are the ability of sterically demanding ligands such as $P(o\text{-tolyl})_3$ to promote coordinative unsaturation and the ability of homochiral bidentate phosphines to control enantioselectivity. Though conformational isomerism in free triarylphosphines has been extensively investigated,[1] much less is known about the stereodynamics of metal phospine complexes. As a contribution to the developing interest in this subject,[2] we wish to report here our studies on the $Fe(CO)_4L$ series (**1a–d**) where L is $P(o\text{-tolyl})_3$, $As(o\text{-tolyl})_3$, $P(o\text{-tolyl})_2CH_2Ph$, and $(o\text{-tolyl})_2PP(o\text{-tolyl})_2$. Part of this work has been reported as a preliminary communication.[3]

Results and Discussion

Complexes **1a,b** were prepared by reaction of $Fe_2(CO)_9$ with the free ligand. Complexes **1c,d** result from our fortuitous discovery that $P(o\text{-tolyl})_3$ undergoes facile photolytic P–C bond cleavage in toluene to produce $P(o\text{-tolyl})_2CH_2Ph$ and $(o\text{-tolyl})_2PP(o\text{-tolyl})_2$. Though photolysis of PPh_3 alone is known to produce the PPh_2 radical as the primary photoproduct,[4] we are not aware of any instance where this is competitive with CO substitution when irradiation is done in the presence of a metal carbonyl. Photolysis of $P(o\text{-tolyl})_3$ ($\delta(^{31}P)$ −29.1 ppm) in toluene using a mercury lamp (254 nm) proceeds to completion in 4 h to give an approximately 1:1 mixture of $P(o\text{-tolyl})_2CH_2Ph$ (−30.9 ppm) and $(o\text{-tolyl})_2PP(o\text{-tolyl})_2$ (−35.3 ppm). In benzene, a slower reaction yields only $(o\text{-tolyl})_2PP(o\text{-tolyl})_2$, indicating that $P(o\text{-tolyl})_2CH_2Ph$ is derived from reaction of the $(o\text{-tolyl})_2P$ radical with solvent. Neither phosphine has been previously reported.[5] Because of oxidative instability and difficulties in separation, the mixture was reacted with excess $Fe_2(CO)_9$ to give **1c,d** which were separated by chromatography.

In all cases, variable-temperature NMR spectroscopy identifies restricted P–C rotation as the process of highest energy, with no evidence of restricted M–P rotation.[6] This is in contrast to several studies of PPh_3 complexes where M–P rotation is the process of highest energy.[2a,c,7]

(a) $Fe(CO)_4P(o\text{-tolyl})_3$ and $Fe(CO)_4As(o\text{-tolyl})_3$ (1a,b). Complexes **1a,b** are isostructural (Figure 1) and reveal a trigonal bipyramidal structure which deviates little from idealized geometry; $Fe(CO)_4PPh_3$ exhibits similar structural features.[8] The phosphine and arsine adopt an exo_3 conformation[9] in which the methyl group of the *o*-tolyl moiety approximately bisects the equatorial CO–Fe–CO angles. In **1b**, the longer Fe–As and As–C bonds, together with a slightly contracted C–As–C angle, indicate less steric interaction of the equatorial carbonyls with the *o*-tolyl substituents. The single a_1 vibrations observed for **1a,b**, respectively, at 2043 and 2047 cm^{-1} (hexane) indicate that only the axial isomer is populated in solution.[10]

In solution at 183 K, the ^{31}P NMR spectrum of **1a** is resolved into two resonances in the ratio 7:1 (Figure 2) which may be assigned to the exo_3 (major) and exo_2 (minor) isomers, respectively, on the basis of the ^1H NMR spectrum at 180 K, which in the methyl region exhibits a single major resonance assignable to exo_3 and three minor resonances of equal intensity assignable to exo_2. Line shape analysis of the ^{31}P spectrum yields the rates and activation parameters shown in Table I. The lowest energy

‡ University College.
† Keele University.
§ Bar Ilan University.

(1) (a) Mislow, K. *Chemtracts: Org. Chem.* **1989**, *2*, 151. (b) Mislow, K. *Acc. Chem. Res.* **1976**, *9*, 26.
(2) For recent articles, see: (a) Davies, S. G.; McNally, J. P.; Derome, A. E. *J. Am. Chem. Soc.* **1991**, *113*, 2854. (b) Casey, C. P.; Whitaker, G. T.; Campana, C. F.; Powell, D. R. *Inorg. Chem.* **1990**, *29*, 3376. (c) Chudek, J. A.; Hunter, G.; Mackay, R. L.; Kremmingher, P.; Schlogl, K.; Weissensteiner, W. *J. Chem. Soc., Dalton Trans.* **1990**, 2001. (d) Brown, T. L. *Inorg. Chem.* **1992**, *31*, 1286.
(3) Howell, J. A. S.; Palin, M. G.; McArdle, P.; Cunningham, D.; Goldschmidt, Z.; Gottlieb, H. E.; Hezroni-Langerman, D. *Inorg. Chem.* **1991**, *30*, 4685.
(4) (a) Otrebski, W.; Getoff, N.; Wilke, G. *Radiat. Phys. Chem.* **1984**, *23*, 691. (b) Islam, T. S. A.; Ferdowsi, F.; Mahmood, A. J.; Hossain, M. A. *J. Bangladesh Acad. Sci.* **1990**, *14*, 63.
(5) Closest relatives are $As(o\text{-tolyl})_2CH_2Ph$ (Gigauri, R. D.; Indzhiya, M. A.; Chernokalski, B. D.; Ugulara, M. M. *Zh. Obshch. Chim.* **1975**, *45*, 2179) and $(p\text{-tolyl})_2PP(p\text{-tolyl})_2$ (Negoiu, D.; Lupu, D. *Chem. Abstr.* **1973**, *79*, 78886a).
(6) For evidence of restricted P–C rotation in the $XP(o\text{-tolyl})_3$ series (X = O, S, Se) see: Howell, J. A. S.; Palin, M. G.; McArdle, P.; Cunningham, D.; Goldschmidt, Z.; Gottlieb, H. E.; Hezroni-Langerman, D. *J. Chem. Soc., Perkin Trans. 2* **1992**, 1769.
(7) Docherty, J. B.; Rycroft, D. S.; Sharp, D. W. A.; Webb, G. A. *J. Chem. Soc., Chem. Commun.* **1979**, 336.
(8) Riley, P. E.; Davis, R. E. *Inorg. Chem.* **1980**, *19*, 159.
(9) If a regular trigonal pyramid is constructed from the metal as apex and the three para ring carbons as base, a proximal (exo) substituent will point away from the base, while a distal (endo) substituent will point toward the base. The terms exo_3 and exo_2 define the number of proximal ortho methyl groups.
(10) Martin, L. R.; Einstein, F. W. B.; Pomeroy, R. K. *Inorg. Chem.* **1985**, *24*, 2777.

0020-1669/93/1332-3493$04.00/0

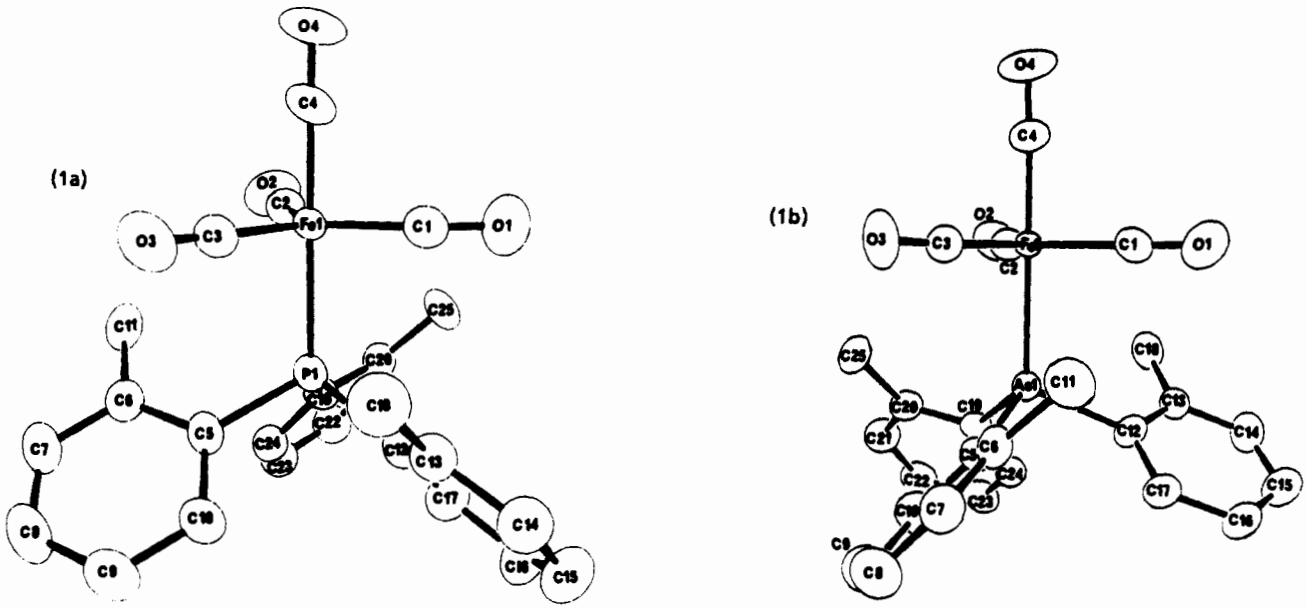

Figure 1. Molecular structures of **1a,b**. Important bond lengths (Å) and angles (deg) for **1a,b** respectively: Fe–P/As = 2.306(1), 2.393(1); Fe–CO_{eq}(av) = 1.763(5), 1.787(7); Fe–CO_{ax} = 1.777(6), 1.772(7); P/As–C(av) = 1.849(4), 1.967(6); CO_{ax}–Fe–CO_{eq}(av) = 89.4(3), 90.2(3); P/As–Fe–CO_{ax}(av) = 90.6(2), 89.8(2); C–P/As–C(av) = 103.3(2), 101.9(2); CO_{eq}–Fe–CO_{eq}(av) = 120.0(2), 120.0(3); Fe–P/As–C_{ipso}–C_{Me}(av) = 53, 52.

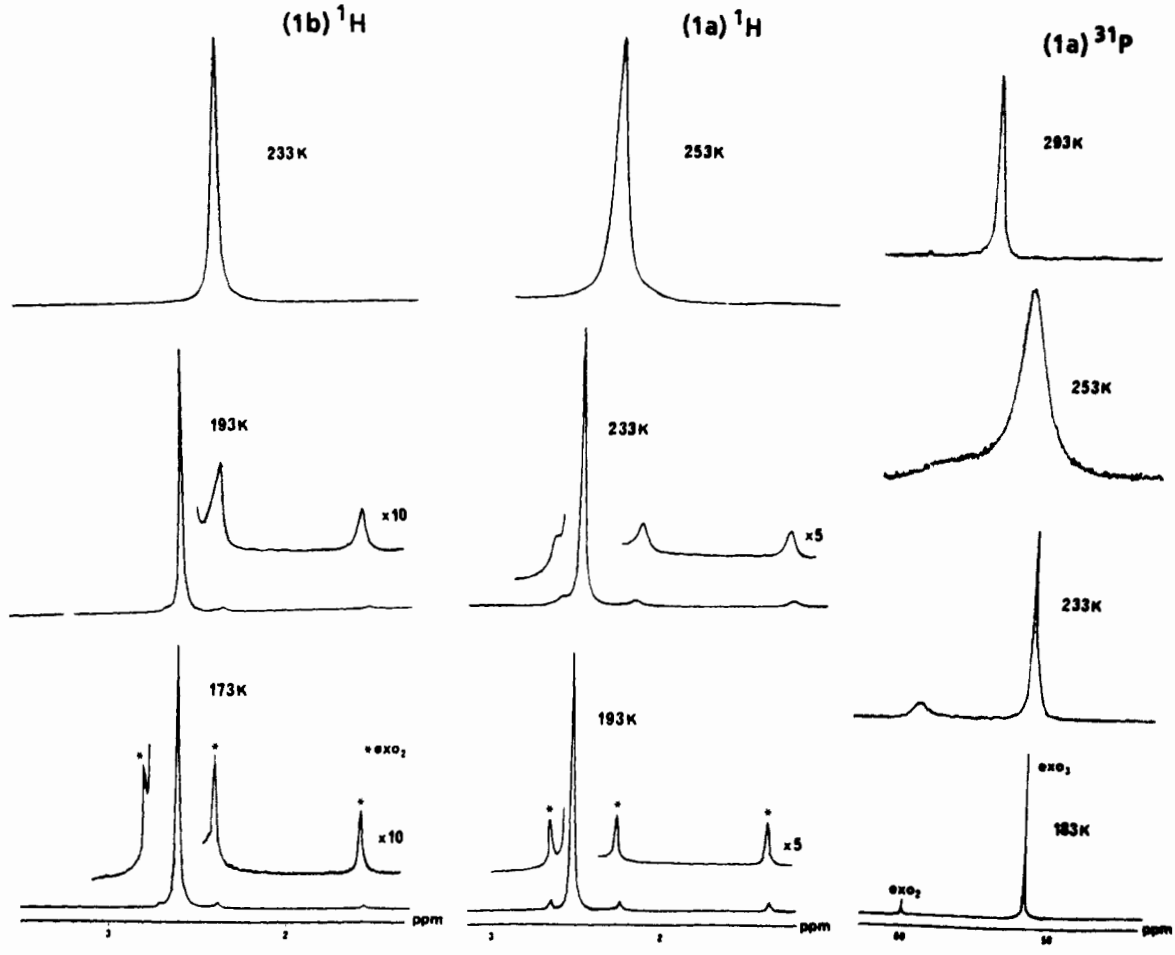

Figure 2. ^{1}H and ^{31}P NMR spectra of **1a,b**.

pathway which results in exo_2/exo_3 interchange and consequent ring exchange in the exo_2 isomer is the "two-ring-flip" mechanism represented in Scheme I.[19]

Of more interest are the ^{13}C spectra of **1a** (Figure 3), which reveal a dependence of intramolecular CO exchange on phosphine conformation. The room-temperature resonance is replaced at 198 K by two resonances in the ratio 3:1 which are clearly assignable to the equatorial and axial carbonyls of the major exo_3 isomer, together with a single broadened resonance assignable to exo_2 which broadens further but remains unresolved at lower temperature. It may be noted that J(P–CO_{ax}) and J(P–CO_{eq}) are of opposite sign; this has also been demonstrated for the cis/trans couplings in some $M(CO)_4P_2$ complexes (M = Mo, W).[11]

As far as we are aware, this represents the first observation of a limiting low-temperature spectrum for a pentacoordinate Fe-

(11) Colquhoun, I. J.; Grim, S. O.; McFarlane, W.; Mitchell, J. D.; Smith, P. H. *Inorg. Chem.* **1981**, *20*, 2516.

Table I. Rates and Activation Parameters

process	temp/K	rate const/s^{-1}	$\Delta G^{\ddagger}$/kJ mol^{-1}
exo$_2$ → exo$_3$ exchange	213	45	44.8
in **1a**	233	480	44.6
	253	2200	45.4
	273	10700	45.6
	293	33000	46.3
ax/eq exchange	178	2	41.8
in exo$_3$(**1a**)	198	50	41.3
	213	340	41.2
	233	3000	41.0
	253	24000	40.4
	293	470000	39.8
ax/eq exchange	178	6600	29.8
in exo$_2$(**1a**)	198	40000	30.3
	213	300000	29.2
exo$_2$ → exo$_3$ exchange	173	3	39.9
in **1b**	193	32	41.0
	213	250	41.7
	233	3500	40.8
	253	20000	40.8
ring exchange	213	5	48.6
in **1c**	233	60	48.6
	253	500	48.4
	273	3000	48.4
D → C exchange	178	200	35.0
in **1d**	193	1500	34.8
	213	11000	35.1
B → A exchange	193	20	40.2
in **1d**	213	50	40.3
	233	360	41.1
D → B exchange	233	1300	42.6
in **1d**	253	10000	42.2
	273	45000	42.3
	293	250000	41.4
C → A exchange	233	800	43.5
in **1d**	253	6000	43.2
	273	29000	43.3
	293	170000	42.2

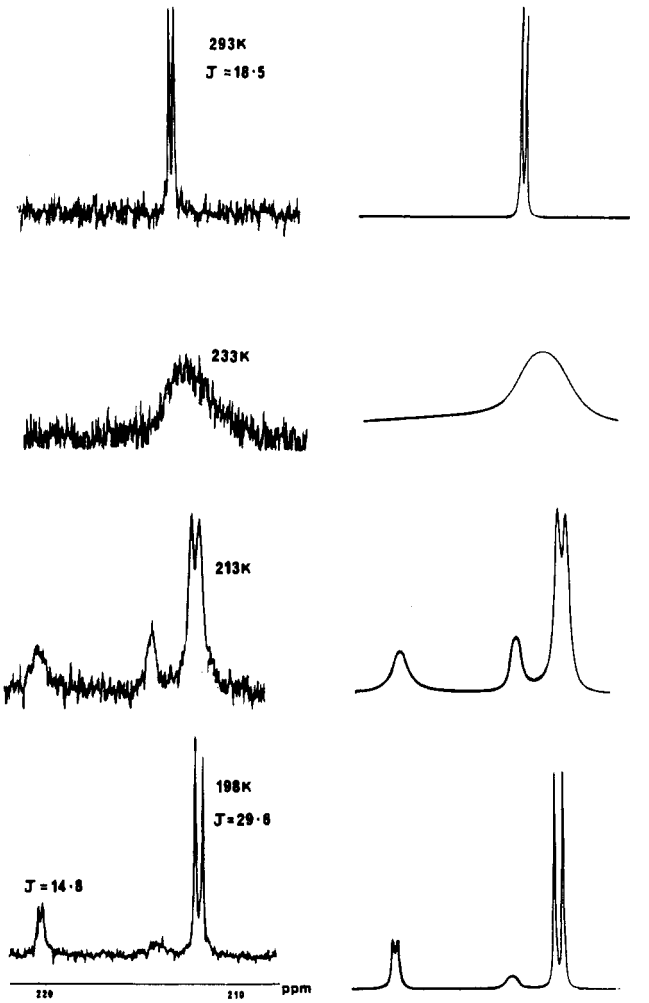

Figure 3. Experimental and simulated ^{13}CO spectra of **1a**.

Scheme I

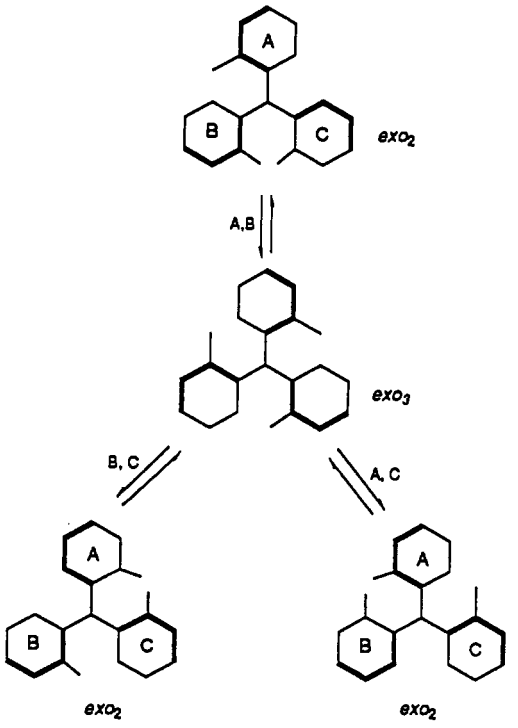

(CO)$_4$L complex containing a simple longitudinal ligand. Though ^{13}CO spectra of (alkene)Fe(CO)$_4$ complexes may also be resolved at low temperature, there are indications that metal–alkene rotation and axial/equatorial CO exchange are interdependent for electronic reasons.[12]

Line shape analysis shows the barrier to axial/equatorial CO exchange to be approximately 13 kJ mol^{-1} less in the exo$_2$ conformation. Thus, though the exo$_3$ conformer is thermodynamically most stable, the barrier to axial/equatorial exchange is lower in the exo$_2$ conformer. Analysis of the Berry pseudorotation pathway indicates that an equatorial Fe(CO)$_4$L isomer lies at or near the transition state, and molecular modeling (see Experimental Section) reveals a considerably lower energy for superposition of a C_1 (exo$_2$) rather than C_3 (exo$_3$) conformation on an equatorial C_{4v} Fe(CO)$_4$ fragment (Figure 4). The similarity of the barrier for axial/equatorial exchange in the exo$_3$ conformation to the barrier for exo$_2$/exo$_3$ interconversion may be noted. Thus, the two processes either may be correlated or may be represented as a cascade in which rate-limiting exo$_2$/exo$_3$ exchange is followed by relatively rapid axial/equatorial CO exchange.

The ^{1}H and ^{13}C NMR spectra of **1b** at low temperature are similar (Figure 2). The exo$_3$:exo$_2$ ratio has increased from 7:1 to 13:1; line shape analysis of the ^{1}H spectra yields a $\Delta G^{\ddagger}_{213}$ of 42 kJ mol, slightly less than the value for **1a** of 45 kJ mol^{-1} and consistent with the reduced steric demands of As(*o*-tolyl)$_3$ as revealed in the solid-state structure. Low intensity of the exo$_2$ resonance precludes line shape analysis of the ^{13}C spectra, but the appearance at 193 K is broadly similar to that of **1a**, namely well-resolved axial/equatorial resonances for the exo$_3$ isomer together with a single broadened resonance assignable to exo$_2$.

(12) (a) Albright, T. A.; Hoffmann, R.; Thibeault, J. C.; Thorn, D. L. *J. Am. Chem. Soc.* **1979**, *101*, 3801. (b) Rossi, A. R.; Hoffmann, R. *Inorg. Chem.* **1975**, *14*, 365.

Table II. NMR Data for **1a–d**[a]

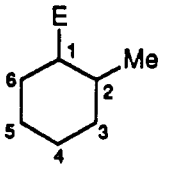

complex	^1H[b]		^{13}C[c]		^{31}P[d]	
1a	3–6	7.1–7.5 (m)	1	129.8 (43)		53.0
	Me	2.48	2	143.2 (11)		
			4	131.1		
			5	125.9 (9)		
			3, 6	132.0		
			Me	23.9		
			CO	214.6 (18)		
1b	3–6	6.9–7.5 (m)	1	131.2		
	Me	2.53	2	142.6		
			4	131.0		
			5	126.4		
			3, 6	132.2		
				132.3		
			Me	22.7		
			CO	214.0		
1c	3–6, Ph	6.7–7.9 (m)	2	140.3 (24)		78.9
	Me	2.05	1, 3–6, Ph	126–137		
	CH_2	4.06 (10.3)	CH_2	38.7 (24)		
			Me	22.1 (4)		
			CO	213.5 (17)		
1d[e]	3–6, 3′–6′	7.0–7.7 (m)	1–6, 1′–6′	125–143	P′	−18.7
	Me, Me′	1.91	Me, Me′	20.4 (22)	P	49.8 (277)
		1.53		22.1		
			CO	216.2 (8)		
$(CO)_4FePh_2PPPh_2$[e]	2–6, 2′–6′	6.9–7.8 (m)	1–6, 1–6′	128–136	P′	3.5
			CO	213 (16.5)	P	61.6 (323)

[a] CD_2Cl_2 solvent, 293 K. [b] ppm from TMS; J(P–H) in parentheses. [c] ppm from TMS; J(P–C) in parentheses. [d] ppm from 85% H_3PO_4; J(P–P) in parentheses. [e] Prime refers to uncoordinated PR_2 moiety.

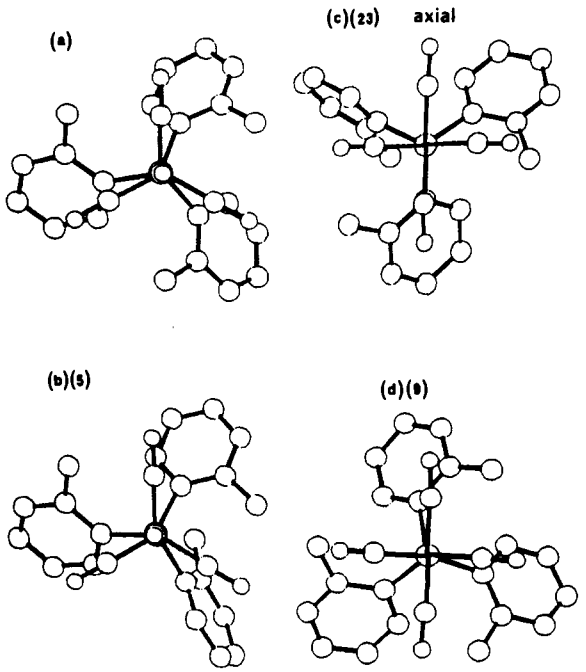

Figure 4. Lowest energy conformations of **1a** (views along M–P bond; metal and hydrogens omitted): (a) crystal structure; (b) axial phosphine, minimized exo_2 conformation; (c) equatorial phosphine, minimized exo_3 conformation; (d) equatorial phosphine, minimized exo_2 conformation. Numbers in parentheses indicate energy (kcal) relative to (a).

(b) $Fe(CO)_4P(o\text{-tolyl})_2CH_2Ph$ (1c). A single-crystal structure determination of **1c** (Figure 5) reveals an axially coordinated phosphine in which the C_{ipso} and CH_2 carbons approximately bisect the equatorial CO–Fe–CO angles. These angles are rather asymmetric, with C(1)–Fe–C(3) expanded to 129° to accommodate the distal *o*-tolyl ring. Though not of the same magnitude, similar distortions have been observed in other axial $Fe(CO)_4PR_3$ complexes.[13]

In solution, a restricted P–C rotational process is evident in the transformation of the singlet Me and doublet CH_2 resonances to doublet and AX systems, respectively, at low temperature (Figure 5). These observations require as a minimum a restricted rotation about the P–C_{ipso} bonds and provide no information on possible restricted rotation about the P–CH_2 bond. Line shape analysis using single rate constants (Table I) fits both Me and CH_2 resonances; the ΔG^*_{273} value for ring exchange of 49 kJ mol^{-1} is similar to the ΔG^*_{273} value of 48 kJ mol^{-1} for ring exchange in **1a**. The ^{13}C resonance is broadened but not resolved at 173 K, similar to the spectrum of the exo_2 isomer of **1a**.

(c) $(CO)_4Fe(o\text{-tolyl})_2PP(o\text{-tolyl})_2$ (1d).[15] A single-crystal structure determination (Figure 6) reveals a distorted trigonal bipyramid with η^1-coordination of the diphosphine in an equatorial position. While both *o*-tolyl groups are proximal on P(2), one is distal on P(1). The methyl of the proximal *o*-tolyl bisects the C(4)–Fe–C(3) angle, while P(2) and the ipso carbon of the distal *o*-tolyl bisect C(1)–Fe–C(2) and C(2)–Fe–C(3) respectively. The uncoordinated P(*o*-tolyl)$_2$ moiety is extended into the space formed by the larger of the two P–Fe–CO_{eq} angles. Though relatively rare, other equatorially substituted $Fe(CO)_4P$ complexes show similar, though smaller, distortions from idealized geometry.[16] The orientation of the putative lone pair on P(2) and the Fe(CO)$_4$ fragment on P(1) is trans. Tetramesityldiphosphine is also trans,[17] and while tetramethyldiphosphine exists as a trans/

(13) (a) Dias Rodriguez, A. M. G.; Lechat, J. R.; Francisco, R. H. P. *Acta Crystallogr.* **1992**, *48C*, 159. (b) Pickardt, J.; Rosch, L.; Schumann, H. *J. Organomet. Chem.* **1976**, *107*, 241. (c) Kilbourn, B. T.; Raeburn, U. A.; Thompson, D. T. *J. Chem. Soc. A* **1969**, 1906.

(14) (a) $Cr(CO)_5P(o\text{-tolyl})_3$: 70, 60, 0° (ref 3). (b) $SeP(o\text{-tolyl})_3$: 59, 56, 13° (Cameron, T. S.; Dahlen, B. *J. Chem. Soc., Perkin Trans. 2* **1975**, 1737).

(15) For a recent review of R_2PPR_2 metal complexes, see: Caminade, A. M.; Majoral, J. P.; Mathieu, R. *Chem. Rev.* **1991**, *91*, 575.

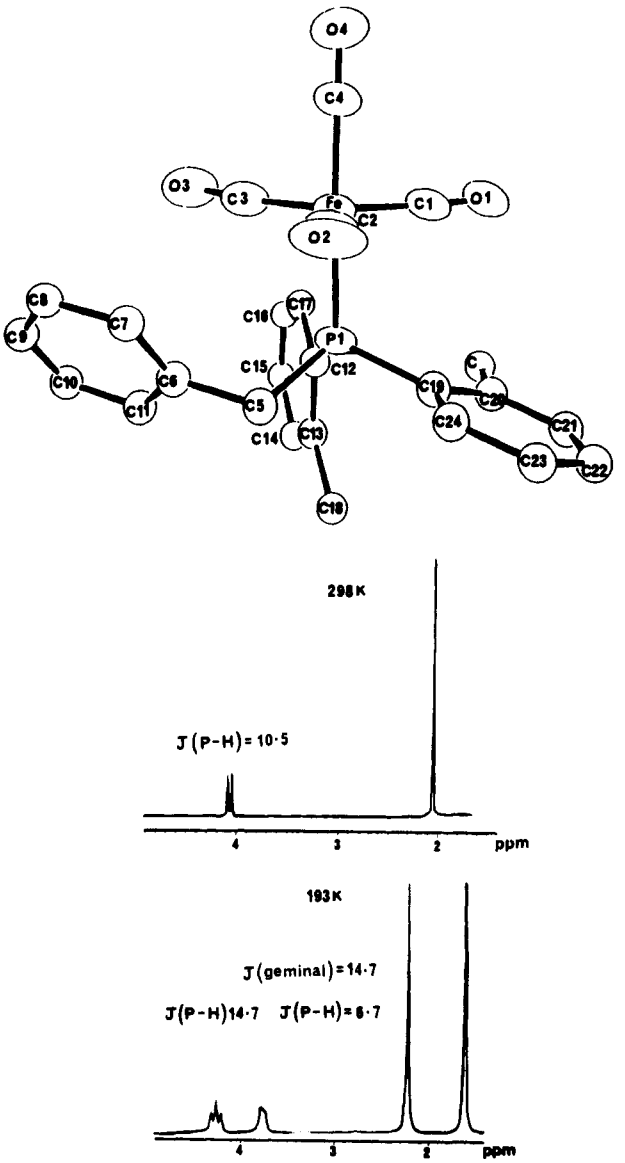

Figure 5. Molecular structure and NMR spectra of **1c**. Important bond lengths (Å) and angles (deg): Fe–P = 2.271(2), Fe–CO_{eq}(av) = 1.783(7), Fe–CO_{ax} = 1.780(7), P–C(av) = 1.850(6), P–Fe–CO_{eq}(av) = 90.2(2), CO_{ax}–Fe–CO_{eq}(av) = 89.9(3), P–Fe–C(4) = 176.3(2), C(2)–Fe–C(1) = 115.1(3), C(3)–Fe–C(1) = 129.2(3), C(3)–Fe–C(2) = 115.7(3), C(12)–P–C(5) = 103.5(3), C(19)–P–C(5) = 103.3(3), C(19)–P–C(12) = 108.2(2), P–C(5)–C(6) = 113.6(4), Fe–P–C(12)–C(13) = 180, Fe–P–C(19)–C(20) = 94.

gauche mixture,[18] crystal structure studies of $(CO)_nM_2(P_2R_4)$ (n = 6, M = Ni, R = Ph; n = 8, M = Fe, R = Me) reveal trans configurations.[19] The P–P bond length (2.24 Å) is similar to that in $[Ni(CO)_3]_2P_2Ph_4$ (2.28 Å)[19] but shorter than that in tetramesityldiphosphine (2.36 Å).[17]

In hexane solution, two a_1 vibrations of approximately equal intensity at 2043 and 2055 cm^{-1} are observed, consistent with an

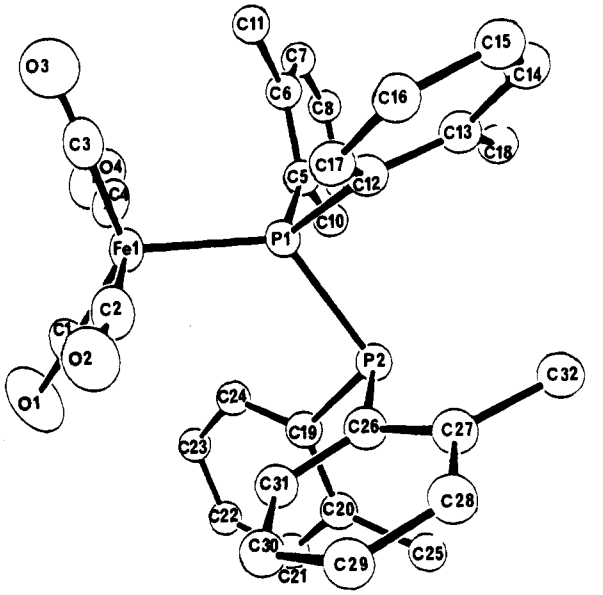

Figure 6. Molecular structure of **1d**. Important bond lengths (Å) and angles (deg): Fe–P(1) = 2.301(2), Fe–CO(av) = 1.78(1), P(1)–P(2) = 2.244(3), P(1)–C(av) = 1.848(8), P(2)–C(av) = 1.843(7), Fe–P(1)–C(5)–C(6) = 72, Fe–P(1)–C(12)–C(13) = −160, lp–P(2)–C(19)–C(20) = 61, lp–P(2)–C(26)–C(27) = 20, lp–P(2)–P(1)–Fe = 176, C(2)–Fe–C(4) = 165.7(4), C(1)–Fe–C(3) = 131.9(4), P(1)–Fe–C(3) = 108.5(3), P(1)–Fe–C(1) = 119.5(3), C(2)–Fe–P(1) = 101.9(3), C(4)–Fe–P(1) = 92.2(3), C_{ax}–Fe–C_{eq}(av) = 87.2(4), Fe–P(1)–P(2) = 122.2(1), C–P–C(av) = 102.9(3), Fe–P(1)–C(5) = 111.3(3), Fe–P(1)–C(12) = 117.4(2).

equilibrium of equatorial and axial isomers. Though such equilibria have been observed for $Ru(CO)_4(EPh_3)$ (E = As, Sb) and $Os(CO)_4SbPh_3$,[10] this represents the first example of such an equilibrium in the iron series.

NMR spectra (Figure 7) also reveal a P–C restricted rotational process. At low temperature, both the coordinated and noncoordinated ^{31}P resonances are resolved into four unequal doublets. Line shape analysis of the coordinated-phosphorus region yields the rates and activation parameters shown in Table I. Though the number of potential conformers is large, only four are energetically accessible if the reasonable assumptions are made (a) that, with respect to the P–P bond, only trans conformers are populated and (b) that, with respect to the P–C bonds, conformers containing two distal rings on the same phosphorus or two distal rings in a gauche configuration on adjoining phosphorus atoms are discounted.[20]

Isomer **i** is that observed in the solid state and is tentatively assigned to resonance A, the major isomer in solution. The four

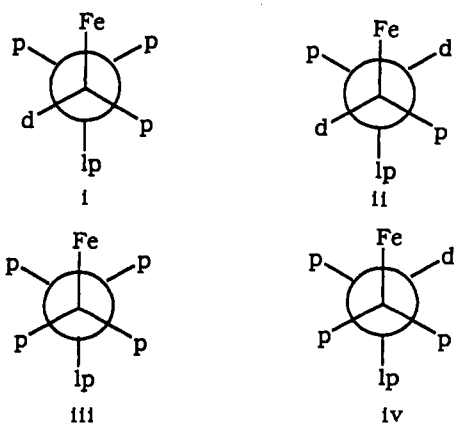

p = proximal d = distal lp = lone pair

(16) (a) Neilson, R. H.; Thoma, R. J.; Vickovic, I.; Watson, W. H. *Organometallics* **1984**, *3*, 1133. (b) Sheldrick, W. S.; Morton, S.; Stelzer, O. *Z. Anorg. Allg. Chem.* **1981**, *475*, 232. (c) Flynn, K. M.; Olmstead, M. M.; Power, P. P. *J. Am. Chem. Soc.* **1983**, *105*, 2085. (d) Cowley, A. H.; Kildutt, J. E.; Lasch, J. G.; Norman, N. C.; Pakulski, M.; Ando, F.; Wright, T. C. *J. Am. Chem. Soc.* **1983**, *105*, 7751.
(17) Baxter, S. G.; Cowley, A. H.; Davies, R. E.; Riley, P. E. *J. Am. Chem. Soc.* **1981**, *103*, 1699.
(18) (a) Durig, J. R.; DiYorio, J. S. *Inorg. Chem.* **1969**, *8*, 2796. (b) Ames, D. L.; Turner, D. W. *J. Chem. Soc., Chem. Commun.* **1975**, 179. (c) Schuweig, A.; Thon, N.; Vermeer, H. *J. Am. Chem. Soc.* **1979**, *101*, 80. (d) Cowley, A. H.; Dewar, M. J. S.; Goodman, D. W.; Padolina, M. C. *J. Am. Chem. Soc.* **1974**, *96*, 2648.
(19) (a) Jarvis, J. A. J.; Mais, R. H. B.; Owston, P. G.; Thompson, D. T. *J. Chem. Soc. A* **1968**, 622. (b) Mais, R. H. B.; Owston, P. G.; Thompson, D. T.; Wood, A. M. *J. Chem. Soc. A* **1967**, 1745.
(20) Modeling using CHEM-X of an all-distal (o-tolyl)$_2$P$_2$ fragment (∠C–P–P = 95°, ∠lp–P–C_{ipso}–C(Me) = 165°] with energy minimization about the C–Me bond shows that the gauche isomer is less stable than the trans by at least 8 kJ.

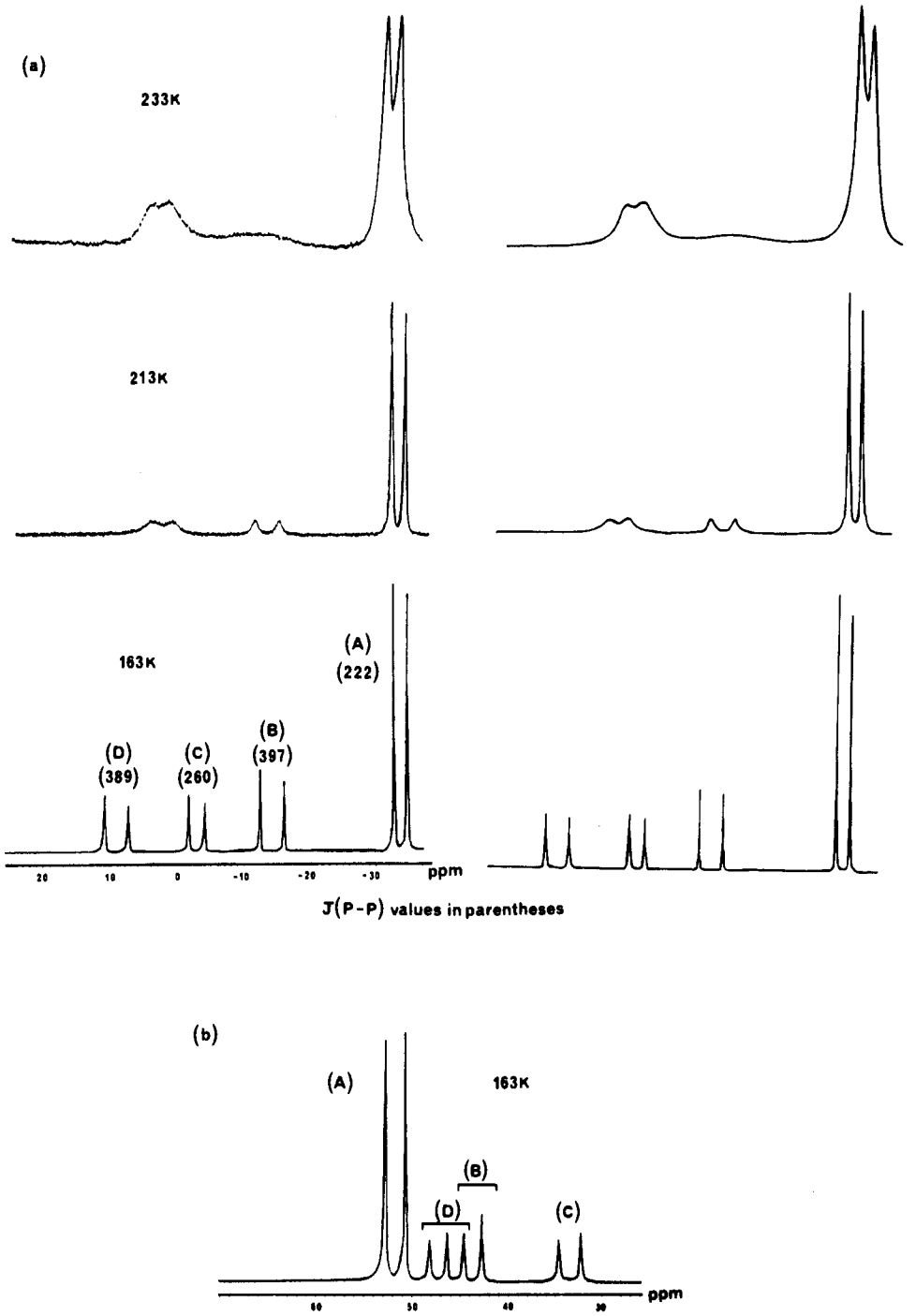

Figure 7. ^{31}P NMR spectra of **1d**: (a) experimental and simulated spectra of uncoordinated phosphorus; (b) experimental spectrum of coordinated phosphorus.

interconversions for which rate constants are defined experimentally are most likely to be those requiring rotation about only one P–C bond; **i** ↔ **iv** and **ii** ↔ **iii** interconversions require two P–C bond rotations and probably represent processes of higher energy.

We ascribe the differing P–P coupling constants (222, 260 Hz versus 397, 389 Hz) to occupancy by phosphorus of the equatorial and axial sites of the trigonal bipyramid, respectively. The complex $(CO)_4Fe(Ph_2PPPh_2)$, which most certainly contains axial phosphine, has a coupling constant of 323 Hz.

The temperature dependence of the ^{13}CO subspectrum is also consistent with this interpretation. On the basis of the spectra of **1a**, one would expect for the averaged spectrum of a P-equatorial isomer a resonance with a near-zero coupling constant, whereas for a P-axial isomer a resonance with a coupling constant of ca. 18 Hz would be anticipated with a chemical shift ordering of P-equatorial > P-axial.[21] $(CO)_4Fe(Ph_2PPPh_2)$ exhibits a single temperature-independent resonance at 213 ppm with J(P–C) = 16 Hz together with a smaller coupling of 5 Hz to the uncoordinated phosphorus. For **1d** (Figure 7), the single room-temperature doublet (216.3 ppm, J = 8 Hz) is replaced at 183 K by two resonances at 217 (J = 5 Hz) and 213 ppm (broadened) in the ratio 2.2:1, consistent with slow exchange among conformers **i**–**iv** but with axial/equatorial CO exchange remaining fast on the NMR time scale in each conformer. Below 183 K, the resonance at 213 ppm selectively broadens, indicating slowing of the axial/equatorial exchange process in the axial isomers. The combined ratio of (A + C) = (B + D) of 2.0:1 obtained from the low-temperature ^{31}P spectrum is close to the ratio of the two ^{13}CO resonances at low temperature (2.2:1).

(21) $(CO)_4FePPh_3$, in which PPh_3 is axial, exhibits a temperature-independent doublet at 209.1 ppm (J = 18 Hz).

Table III. Crystallographic Data for **1a–d**

	1a	**1b**	**1c**	**1d**
chem formula	$C_{25}H_{21}FeO_4P$	$C_{25}H_{21}AsFeO_4$	$C_{25}H_{21}FeO_4P$	$C_{32}H_{28}FeO_4P_2$
fw	472.28	516.20	472.28	594.37
space group	$P2_1/n$	$P2_1/n$	$P\bar{1}$	$Pbca$
a/Å	10.188(3)	10.265(2)	9.618(3)	15.947(6)
b/Å	10.429(2)	10.517(1)	15.282(3)	20.009(3)
c/Å	21.755(6)	21.679(3)	17.130(5)	18.470(4)
α/deg			66.92(2)	
β/deg	99.79(2)	99.16(2)	79.51(2)	
γ/deg			86.42(2)	
Z	4	4	4	8
μ/cm^{-1}	7.60	21.0	6.99	6.00
V/Å^3	2277	2310	2292	5893
ρ/g cm^{-3}	1.38	1.48	1.37	1.34
λ/Å	0.7093	0.7093	0.7093	0.7093
temp/°C	22	22	22	22
R	0.0520	0.0495	0.0643	0.0589
R_w	0.0573	0.0521	0.0773	0.0669

These results thus demonstrate a much higher stereochemical rigidity in these *o*-tolyl derivatives compared to their phenyl counterparts. The possible use of homochiral *o*-tolyl-functionalized mono- and bidentate phosphines as enantioselective catalysts is under investigation.

Experimental Section

NMR spectra were recorded using a JEOL GSX 270 spectrometer; temperatures were measured using the in-built copper–constantan thermocouple. Line shape analyses were performed using the EXCHANGE program (R. E. D. McClung, University of Alberta). P(*o*-tolyl)$_3$,[22] As(*o*-tolyl)$_3$,[6] and (CO)$_4$FePh$_2$PPPh$_2$[23] were prepared by literature methods. Solvents were dried and degassed before use.

(i) Synthesis of (1a,b). $Fe_2(CO)_9$ (3 g, 8.25 mmol) and P(*o*-tolyl)$_3$ (2.5 g, 8.25 mmol) in diethyl ether (50 mL) were refluxed for 1 h. After filtration and evaporation of solvent, the crude product was purified by chromatography (grade II alumina, diethyl ether) to give the product **1a** (2.5 g, 64%). Crystals for structure determination were grown from ethyl acetate. Complex **1b** was prepared similarly.

Anal. Calc for **1a**: C, 63.6; H, 4.45. Found: C, 63.2; H, 4.38. Mp: 165–166 °C dec. Infrared (hexane): 2043, 1975, 1947 cm^{-1}.

Anal. Calc for **1b**: 58.2; H, 4.10. Found: C, 58.2; H, 4.03. Mp: 173 °C dec. Infrared (hexane): 2047, 1971, 1943 cm^{-1}.

(ii) Synthesis of (1c,d). P(*o*-tolyl)$_3$ (2.5 g, 8.25 mmol) in toluene (230 mL) was irradiated for 4 h using a 90-W Hg arc lamp (254 nm). After filtration through Celite, the solvent was removed to give a white solid (2.2 g) containing a 1:1 mixture of (*o*-tolyl)$_2$PP(*o*-tolyl)$_2$ and P(*o*-tolyl)$_2$CH$_2$Ph.

This mixture (1.7 g) and $Fe_2(CO)_9$ (2.0 g, 5.6 mmol) were refluxed in diethyl ether (50 mL) for 1.5 h. After filtration and removal of solvent, 0.8 g of the residue was purified on a chromatotron (95% bp 60–80 °C petroleum ether/5% ethyl acetate) to give **1d** (340 mg) and **1c** (240 mg) in order of elution. Crystals for both were grown from bp 60–80 °C petroleum ether.

Anal. Calc for **1c**: C, 63.6; H, 4.48. Found: C, 63.7; H, 4.51. Mp: 133 °C dec. Infrared (hexane): 2047, 1971, 1955, 1935 cm^{-1}.

Anal. Calc for **1d**: C, 64.6; H, 4.71. Found: C, 64.6; H, 4.71. Mp: 115–116 °C. Infrared (hexane): 2055, 2043, 1975 (br), 1947 (br) cm^{-1}.

(iii) Crystallographic Results. Data were collected on an Enraf-Nonius CAD4F diffractometer. The structures were solved by direct methods (SHELX86)[24] and refined by full-matrix least-squares procedures (SHELX76).[25] Hydrogen atoms were included in calculated positions with fixed thermal parameters. For **1a,b** all non-hydrogen atoms were refined anisotropically; for **1c,d** only the iron, phosphorus, and atoms of the CO groups were refined anisotropically. In **1c**, there are two chemically identical molecules per asymmetric unit. Atomic scattering factors for non-hydrogen and hydrogen atoms and anomalous dispersion correction factors for non-hydrogen atoms were taken from the literature.[26–28] Data were corrected for Lorentz and polarization effects, but not for absorption. All calculations were performed on a VAX 8700 computer. Crystallographic data are listed in Table III, while atomic coordinates are listed in Tables IV–VI. All crystals used were isolated as orange-yellow parallelepipeds.

Table IV. Fractional Atomic Coordinates for **1a**

atom	x	y	z
Fe(1)	0.13450(6)	0.65983(6)	0.40407(3)
P(1)	–0.01327(11)	0.79578(11)	0.34392(5)
O(1)	0.2660(4)	0.6003(5)	0.2984(2)
O(2)	0.2448(5)	0.8662(5)	0.4887(2)
O(3)	–0.0849(4)	0.5001(4)	0.4317(2)
O(4)	0.3236(5)	0.4869(6)	0.4779(3)
C(1)	0.2114(5)	0.6249(5)	0.3391(2)
C(2)	0.1982(5)	0.7878(6)	0.4541(2)
C(3)	–0.0006(5)	0.5653(5)	0.4206(2)
C(4)	0.2489(6)	0.5537(6)	0.4491(3)
C(5)	–0.1828(4)	0.7821(4)	0.3616(2)
C(6)	–0.2103(5)	0.8028(5)	0.4230(2)
C(7)	–0.3392(5)	0.7823(5)	0.4325(3)
C(8)	–0.4394(5)	0.7429(5)	0.3851(3)
C(9)	–0.4149(5)	0.7264(5)	0.3262(3)
C(10)	–0.2881(4)	0.7478(4)	0.3141(2)
C(11)	–0.1085(6)	0.8456(6)	0.4770(2)
C(12)	–0.0363(4)	0.7712(4)	0.2582(2)
C(13)	–0.0625(4)	0.6486(4)	0.2307(2)
C(14)	–0.0706(5)	0.6412(5)	0.1653(3)
C(15)	–0.0608(6)	0.7459(7)	0.1292(2)
C(16)	–0.0405(6)	0.8643(6)	0.1557(2)
C(17)	–0.0280(5)	0.8755(5)	0.2197(2)
C(18)	–0.0845(6)	0.5289(5)	0.2648(3)
C(19)	0.0247(4)	0.9694(4)	0.3506(2)
C(20)	0.1498(5)	0.0179(4)	0.3424(2)
C(21)	0.1673(6)	1.1497(4)	0.3466(2)
C(22)	0.0676(6)	1.2333(5)	0.3567(3)
C(23)	–0.0561(5)	1.1843(5)	0.3627(2)
C(24)	–0.0760(5)	1.0525(4)	0.3600(2)
C(25)	0.2618(5)	0.9381(5)	0.3274(3)

Table V. Fractional Atomic Coordinates for **1b**

atom	x	y	z
As(1)	0.51131(6)	0.69894(6)	0.15505(3)
Fe(1)	0.36152(9)	0.84096(8)	0.09347(4)
O(1)	0.5857(5))	0.9963(5)	0.0688(3)
O(2)	0.2573(6)	0.6365(6)	0.0081(3)
O(3)	0.2317(5)	0.8950(6)	0.2012(3)
O(4)	0.1773(6)	1.0155(7)	0.0210(4)
C(1)	0.4990(7)	0.9350(6)	0.0781(3)
C(2)	0.3013(7)	0.7140(7)	0.0424(3)
C(3)	0.2862(6)	0.8738(6)	0.1603(3)
C(4)	0.2505(7)	0.9472(7)	0.0486(4)
C(5)	0.5375(6)	0.7222(6)	0.2462(3)
C(6)	0.5627(6)	0.8413(6)	0.2738(3)
C(7)	0.5730(7)	0.8489(8)	0.3392(3)
C(8)	0.5612(8)	0.7449(8)	0.3751(3)
C(9)	0.5385(9)	0.6273(9)	0.3469(3)
C(10)	0.5259(7)	0.6151(7)	0.2830(3)
C(11)	0.5867(8)	0.9602(6)	0.2399(4)
C(12)	0.6921(6)	0.7090(6)	0.1371(3)
C(13)	0.7181(5)	0.6908(6)	0.0756(3)
C(14)	0.8479(7)	0.7097(7)	0.0653(4)
C(15)	0.9448(7)	0.7469(7)	0.1125(4)
C(16)	0.9191(6)	0.7645(6)	0.1728(4)
C(17)	0.7928(6)	0.7440(6)	0.1845(3)
C(18)	0.6157(8)	0.6523(7)	0.0216(3)
C(19)	0.4725(6)	0.5150(5)	0.1491(3)
C(20)	0.3490(6)	0.4683(6)	0.1568(3)
C(21)	0.3341(8)	0.3360(6)	0.1544(3)
C(22)	0.4336(8)	0.2544(7)	0.1451(3)
C(23)	0.5561(8)	0.3039(6)	0.1378(3)
C(24)	0.5733(6)	0.4334(6)	0.1402(3)
C(25)	0.2364(6)	0.5495(6)	0.1711(4)

(22) Allman, T.; Goel, R. G. *Can. J. Chem.* **1982**, *60*, 716.
(23) Collman, J. P.; Komoto, R. G.; Siegl, W. O. *J. Am. Chem. Soc.* **1973**, *95*, 2389.
(24) Sheldrick, G. M. SHELX86: A Computer Program for Crystal Structure Determination. University of Gottingen, 1986.
(25) Sheldrick, G. M. A Computer Program for Crystal Structure Determination. University of Cambridge, 1976.
(26) Cromer, D. T.; Mann, J. B. *Acta Crystallogr.* **1968**, *24A*, 321.
(27) Stewart, R. F.; Davidson, E. R.; Simpson, W. T. *J. Chem. Phys.* **1965**, *42*, 3175.
(28) Cromer, D. T.; Liberman, D. J. *J. Chem. Phys.* **1970**, *53*, 1891.

Table VI. Fractional Atomic Coordinates for **1c**

atom	x	y	z
Fe(1)	0.42395(8)	0.68645(5)	0.34342(5)
P(1)	0.58331(14)	0.78433(10)	0.23431(9)
O(1)	0.4227(5)	0.5653(3)	0.2472(3)
O(2)	0.2141(5)	0.8381(3)	0.3103(3)
O(3)	0.5874(5)	0.6698(4)	0.4775(3)
O(4)	0.2291(6)	0.5506(4)	0.4811(4)
C(1)	0.4279(6)	0.6132(4)	0.2837(4)
C(2)	0.2978(6)	0.7797(5)	0.3216(4)
C(3)	0.5263(7)	0.6789(5)	0.4221(4)
C(4)	0.3041(7)	0.6034(5)	0.4274(4)
Fe(2)	0.06131(9)	0.17917(6)	0.20828(5)
P(2)	−0.08453(14)	0.28295(9)	0.24780(9)
O(101)	−0.1155(7)	0.1456(4)	0.1009(4)
O(102)	0.0859(6)	0.0581(4)	0.3859(4)
O(103)	0.2716(5)	0.3331(4)	0.1289(4)
O(104)	0.2529(8)	0.0498(5)	0.1581(5)
C(101)	−0.0529(8)	0.1626(5)	0.1439(5)
C(102)	0.0690(7)	0.1064(4)	0.3177(5)
C(103)	0.1877(7)	0.2731(5)	0.1593(4)
C(104)	0.1786(8)	0.1008(5)	0.1776(5)
C(5)	0.5857(6)	0.9057(4)	0.2347(4)
C(6)	0.6301(6)	0.9078(4)	0.3137(4)
C(7)	0.5289(8)	0.9076(5)	0.3828(5)
C(113)	−0.3672(6)	0.3198(4)	0.3109(4)
C(114)	−0.5108(7)	0.3020(5)	0.3261(4)
C(115)	−0.5598(8)	0.2279(5)	0.3125(5)
C(116)	−0.4726(7)	0.1671(5)	0.2868(5)
C(117)	−0.3288(6)	0.1822(4)	0.2728(4)
C(118)	−0.3224(7)	0.4018(5)	0.3303(5)
C(119)	−0.0214(5)	0.3083(4)	0.3306(3)
C(120)	−0.0597(6)	0.2553(4)	0.4195(4)
C(121)	0.0016(7)	0.2786(5)	0.4766(4)
C(122)	0.0959(7)	0.3524(5)	0.4487(5)
C(123)	0.1347(7)	0.4044(5)	0.3624(4)
C(124)	0.0769(6)	0.3831(4)	0.3038(4)
C(125)	−0.1653(7)	0.1720(5)	0.4568(4)

Table VII. Fractional Atomic Coordinates for **1d**

atom	x	y	z
Fe(1)	0.61031(6)	0.07168(6)	0.43303(6)
P(1)	0.74183(11)	0.08193(11)	0.38667(9)
P(2)	0.76185(12)	0.08874(112)	0.27582(10)
O(1)	0.4649(5)	0.1327(4)	0.3650(4)
O(2)	0.5463(4)	−0.0673(3)	0.3845(3)
O(3)	0.6236(5)	0.0030(5)	0.5639(4)
O(4)	0.6176(5)	0.2138(4)	0.4970(4)
C(1)	0.5227(6)	0.1086(5)	0.3904(5)
C(2)	0.5760(5)	−0.0141(5)	0.4010(4)
C(3)	0.6200(5)	0.0292(5)	0.5120(5)
C(4)	0.6180(5)	0.1579(5)	0.4716(5)
C(5)	0.7970(5)	0.1619(4)	0.4186(3)
C(6)	0.8229(5)	0.1675(5)	0.4851(4)
C(7)	0.8641(6)	0.2306(5)	0.5056(5)
C(8)	0.8787(6)	0.2854(5)	0.4631(5)
C(9)	0.8540(6)	0.2815(5)	0.3970(4)
C(10)	0.8134(5)	0.2196(4)	0.3754(4)
C(11)	0.8122(6)	0.1075(5)	0.5364(5))
C(12)	0.8172(5)	0.0067(4)	0.4022(3)
C(13)	0.9051(5)	0.0134(5)	0.3979(4)
C(14)	0.9539(6)	−0.0474(5)	0.4171(14)
C(15)	0.9174(6)	−0.1106(5)	0.4361(5)
C(16)	0.8318(6)	−0.1184(5)	0.4374(4)
C(17)	0.7824(5)	−0.0587(4)	0.4207(4)
C(18)	0.9520(6)	0.0795(4)	0.3749(4)
C(19)	0.6824(5)	0.1529(4)	0.2435(4)
C(20)	0.6748(6)	0.1577(5)	0.1741(4)
C(21)	0.6171(6)	0.2079(5)	0.1497(6)
C(22)	0.5713(7)	0.2494(6)	0.1898(5)
C(23)	0.5783(6)	0.2481(5)	0.2577(5)
C(24)	0.6375(5)	0.1975(4)	0.2846(4)
C(25)	0.7261(7)	0.1127(6)	0.1275(5)
C(26)	0.7161(5)	0.0007(4)	0.2543(4)
C(27)	0.7685(5)	−0.0584(4)	0.2390(4)
C(28)	0.7315(5)	−0.1244(5)	0.2220(4)
C(29)	0.6451(6)	−0.1329(5)	0.2194(4)
C(30)	0.5948(6)	−0.0751(4)	0.2317(4)
C(31)	0.6295(5)	−0.0083(5)	0.2492(4)
C(32)	0.8614(6)	−0.0533(5)	0.2381(5)

(iv) **Molecular Modeling.** Modeling was performed using CHEM-X.[29] Minimization of **1a** about conformationally mobile bonds (M–P, P–C), using the default parameters reproduces closely the observed ground-state structure. The alternative higher energy structures were generated similarly but restricting the phosphine to either C_3 (exo_3) or C_1 (exo_2) symmetry. The structures of the equatorial exo_3 and exo_2 isomers of **1a** were modeled using CO_{ax}–Fe–CO_{ax} and CO_{eq}–Fe–P angles of 172 and 117°, respectively. Energy differences between conformers are overestimated, since contributions to energy minimization through bond stretching and bending are neglected.

(29) CHEM-X, designed and distributed by Chemical Design Limited, Oxford, England.

Supplementary Material Available: Full tables of crystallographic data, bond lengths, bond angles, hydrogen atom coordinates, and isotropic and anisotropic thermal parameters and ORTEP diagrams for **1a–d** (35 pages). Ordering information is given on any current masthead page.